A poly-reference implementation of the maximum likelihood complex frequencydomain estimator and some industrial applications

Article · January 2004

CITATIONS
15

READS
311

5 authors, including:

Patrick Guillaume
Vrije Universiteit Brussel
411 PUBLICATIONS **6,331** CITATIONS

SEE PROFILE

S. Vanlanduit
University of Antwerp
204 PUBLICATIONS **2,060** CITATIONS

SEE PROFILE

A Poly-reference Implementation of the Maximum Likelihood Complex Frequency-Domain Estimator and some Industrial Applications

Bart Cauberghe, Patrick Guillaume, Peter Verboven, Eli Parloo and Steve Vanlanduit

Vrije Universiteit Brussel (VUB)
Department of Mechanical Engineering (WERK)
Acoustics and Vibration Research Group (AVRG)
Pleinlaan 2, B-1050 Brussels, Belgium
Bart.Cauberghe@vub.ac.be
www.avrg.vub.ac.be

ABSTRACT

A poly-reference implementation of a maximum likelihood frequency domain estimator is proposed to estimate modal parameters and their confidence intervals from both Frequency Response Functions or from power-and cross-spectral densities in the output-only case. The solver is robust to measurement noise, since it uses the noise information on the data as a weighting in its cost function and can handle measurements with a large dynamical range. Several real-life civil, automotive and aerospace case studies are discussed.

1 INTRODUCTION

During the last two decades, there has been a growing interest for system identification for the domain experimental modal analysis (EMA). The vibration in a structure originates from its resonance modes that are inherent properties of the structure. The modes of the structure are determined by its material properties, size and shape and the boundary conditions. The modal model of a structure expresses the dynamical behavior of linear time-invariant mechanical structure as linear combination of different resonance modes. The total structure is defined by its so-called resonance frequencies, damping ratios, mode shapes and participation factors. Engineers are interested in the structural behavior of their designs and prototypes for applications like:

- Model Updating of finite elements by correlating numerical modal parameters with experimental obtained modal parameters to obtain accurate numerical models.
- Damage detection, Quality Control and Structural Health Monitoring to predict critical failures, optimize product quality and to increase safety.
- Vibro-acoustics, since the existence of a vibro-acoustical coupling between structural vibrations and radiated noise is an important aspect for the design process in terms of comfort.
- Forced Response Analysis, Sensitivity Analysis and Substructuring to predict respectively the effects of external forces, to change of modal parameters in function of mass, damping and stiffness and the modal parameters of an assembled structuring starting from the modal parameters of the individual parts.

All these applications have become key technologies in structural dynamics analysis and require accurate modal model identification from measured vibration responses and forces. During the last 5 years research was done to obtain accurate modal models from noisy data sets. In this paper a poly-reference implementation of a Maximum Likelihood Frequency Domain (p-MLFD) estimator is proposed. In the past both a Least Squares Complex Frequency Domain (LSCF) and Maximum Likelihood Frequency Domain (MLFD) estimator based on a scalar matrix-fraction description -better known as a common-denominator model- were proposed [6], [8], [1] for both classical modal analysis and operational modal analysis. The LSCF method results is very clear stabilization diagrams and the MLFD optimizes these LSCF estimates in a Maximum Likelihood sense by using the variances on the data in the cost function. Both methods are successfully applied in automotive, aerospace and civil engineering applications. These methods are optimized for both speed and memory requirements and can handle high system orders (estimating e.g. 100 different modes in a single band estimation). A more profound analysis of these methods and different variants can be found in [15] and their applications to operational modal analysis (OMA) in [11]

It was found that the identified common-denominator model closely fitted the measured frequency response function (FRF) data. Although, when converting this model to a modal model by reducing the residues to a rank-one matrix using the singular value decomposition (SVD), the quality of the fit decreased [1]. This is a serious drawback of common denominator based models, since many applications need a modal model in terms of the natural frequencies, damping ratios, mode shapes and participation vectors. Another theoretically associated drawback of a common denominator model is that closely spaced poles will erroneously show up as a single pole. However, in practise this problem is solved by increasing the model order, which is typically done in EMA.

These two reasons provided the motivation for a poly-reference version of the LSCF method using a so-called right matrix-fraction model [7], [12]. In this approach both the system poles and the participation factors are available from the denominator coefficients. The main advantage of the poly-reference implementation is that the SVD to decompose the residues in mode shapes and participation factors can be avoided and that closely separately poles can be separated more easily.

A disadvantage of the method is that the model order can only be increased in steps of N_i (the number of input forces) and that the method is more sensitive to data inconsistencies like e.g. mass loading effect over different patches [2].

Table 1: Natural frequencies and damping ratios of the subframe

	Common Denominator Model	Right Matrix Fraction model
Least Squares	LSCF[1]	p-LSCF[7],[12]
Maxium Likelihood	MLFD [6],[8]	**p-MLFD**

In this contribution the poly-reference version of MLFD method is presented. The method forces the same right matrix fraction model as the p-LSCF method on the measured data, but in a Maximum Likelihood sense instead of a linear least squares sense. This Maximum Likelihood implementation improves the starting values provided by the p-LSCF method, since the variances and covariances on the FRFs are used as a weighting to make the algorithm consistent and efficient. As a result the p-MLFD method is very adequate to process noisy MIMO measurements for modal analysis applications. Furthermore it is shown that this method is extremely useful for processing highly damped systems like e.g. EMA of a full trimmed car, acoustical measurements, ...

2 RIGHT MATRIX FRACTION MODEL

The relationship between output o ($o = 1, \ldots, N_o$) and all inputs can be modelled in the frequency domain by means of a right matrix-fraction description (RMFD) [14]

$$\mathbf{H_o}(\omega) = \mathbf{N_o}(\omega)\mathbf{D^{-1}}(\omega) \tag{1}$$

with

$$\mathbf{H_o}(\omega) = \left[\begin{array}{cccc} H_{o1}(\omega) & H_{o2}(\omega) & \ldots & H_{oN_i}(\omega) \end{array} \right] \tag{2}$$

$$\mathbf{N_o}(\omega) = \sum_{\mathbf{r=0}}^{\mathbf{n}} \mathbf{\Omega_r}(\omega)\mathbf{N_{or}}(\omega) \tag{3}$$

the numerator row-vector polynomial of order n of output o ($\mathbf{N_o}(\omega) \in \mathbb{C}^{\mathbf{1\times N_i}}$ and N_i the number of inputs) and

$$\mathbf{D}(\omega) = \sum_{\mathbf{r=0}}^{\mathbf{n}} \mathbf{\Omega_r}(\omega)\mathbf{D_r}(\omega) \tag{4}$$

the denominator matrix polynomial ($\mathbf{D}(\omega) \in \mathbb{C}^{\mathbf{N_i} \times \mathbf{N_i}}$) of order n. The elements of the matrix coefficients $\mathbf{D_r}$ and $\mathbf{N_{or}}$ are the parameters to be estimated. For the methods discussed in this paper, a z-domain model is used (i.e. the frequency domain equivalent of a discrete time model) and, by consequence the basis functions are

$$\Omega_r(\omega) = e^{j\omega T_s r} \tag{5}$$

with T_s the sample time. Solving an eigenvalue problem of the companion matrix formed by the denominator coefficients, results in the nN_i poles and their corresponding participation factors. In fact the calculation from the poles and participation factors from the denominator coefficients is similar as in the Least Squares Complex Exponential (LSCE, Proni) algorithm [9], [10].

3 MAXIMUM LIKELIHOOD ALGORITHM

3.1 Cost Function

Assuming that the FRFs referring to different outputs o to be uncorrelated, the (negative) log-likelihood function reduces to

$$K_{ML}(\theta) = \sum_{o=1}^{N_o} \sum_{f=1}^{N_f} \mathbf{E_o}(\theta, \omega_\mathbf{f})^\mathbf{H} \mathbf{C_o}(\omega_\mathbf{f})^{-\mathbf{1}} \mathbf{E_o}(\theta, \omega_\mathbf{f}) \tag{6}$$

with $.^H$ the complex conjugate transpose of a matrix (Hermitian), $\theta = [\ \mathbf{N_{11}} \quad \dots \quad \mathbf{N_{N_o n}} \quad \mathbf{B_1} \quad \dots \quad \mathbf{B_n}\ ]$ and the equation error (a column vector) given by

$$\mathbf{E_o}(\theta, \omega_\mathbf{f}) = \mathbf{H_o}(\omega_\mathbf{f})^\mathbf{T} - \mathbf{D}(\omega_\mathbf{f})^{-\mathbf{T}} \mathbf{N_o}(\omega_\mathbf{f})^\mathbf{T} \tag{7}$$

and $\mathbf{C_o}(\omega_\mathbf{f})$ the covariance matrix of the equation error row vector

$$\mathbf{C_o}(\omega_\mathbf{f}) = \begin{bmatrix} \sigma_{H_{o1}}(\omega_f)^2 & \sigma_{H_{o1}H_{o2}}(\omega_f)^2 & \dots & \sigma_{H_{o1}H_{oN_i}}(\omega_f)^2 \\ \sigma_{H_{o2}H_{o1}}(\omega_f)^2 & \sigma_{H_{o2}}(\omega_f)^2 & \dots & \sigma_{H_{o2}H_{oN_i}}(\omega_f)^2 \\ \vdots & \vdots & \ddots & \vdots \\ \sigma_{H_{oN_i}H_{o1}}(\omega_f)^2 & \sigma_{H_{oN_i}H_{o2}}(\omega_f)^2 & \dots & \sigma_{H_{oN_i}}(\omega_f)^2 \end{bmatrix} \tag{8}$$

The ML estimate of θ is given by minimizing 6. This can be done by means of a Gauss-Newton optimization algorithm, which takes advantage of the quadratic form of the cost function 6. The Gauss-Newton iterations are given by

$$\text{(a) solve } \mathbf{J_m^H J_m vec}(\mathbf{\Delta\Theta_m}) = -\mathbf{J_m^H vec}(\mathbf{E}) \tag{9}$$

$$\text{(b) set } \Theta_{m+1} = \Theta_m + \Delta\Theta_m \tag{10}$$

with the vec operator defined by $vec\left(\begin{bmatrix} a_{11} & a_{21} \\ a_{12} & a_{22} \end{bmatrix}\right) = [\ a_{11} \quad a_{12} \quad a_{21} \quad a_{22}\ ]^T$ and

$$\mathbf{E} = \begin{bmatrix} \mathbf{E_1}(\theta, \omega_\mathbf{1}) \\ \vdots \\ \mathbf{E_1}(\theta, \omega_{\mathbf{N_f}}) \\ \vdots \\ \mathbf{E_{N_o}}(\theta, \omega_\mathbf{1}) \\ \vdots \\ \mathbf{E_{N_o}}(\theta, \omega_{\mathbf{N_f}}) \end{bmatrix} \tag{11}$$

and the Jacobian has the following structure

$$\mathbf{J} = \begin{bmatrix} \mathbf{X_1} & 0 & \dots & 0 & \mathbf{Y_1} \\ 0 & \mathbf{X_2} & \dots & 0 & \mathbf{Y_2} \\ \vdots & & \ddots & & \vdots \\ 0 & 0 & \dots & \mathbf{X_{N_o}} & \mathbf{Y_{N_o}} \end{bmatrix} \tag{12}$$

with

$$\mathbf{X_o} = \begin{bmatrix} \mathbf{X_o}(\omega_1) \\ \vdots \\ \mathbf{X_o}(\omega_{\mathbf{N_f}}) \end{bmatrix} \in \mathbb{C}^{\mathbf{N_f N_i^2} \times \mathbf{n N_i^2}} \tag{13}$$

$$\mathbf{Y_o} = \begin{bmatrix} \mathbf{Y_o}(\omega_1) \\ \vdots \\ \mathbf{Y_o}(\omega_{\mathbf{N_f}}) \end{bmatrix} \in \mathbb{C}^{\mathbf{N_f N_i} \times \mathbf{n N_i}} \tag{14}$$

and

$$\begin{aligned}
\mathbf{X_o}(\omega_\mathbf{f}) &= \begin{bmatrix} \frac{\partial \mathbf{E_o}(\omega_\mathbf{f})}{\partial vec(\mathbf{D_{o1}})} & \frac{\partial \mathbf{E_o}(\omega_\mathbf{f})}{\partial vec(\mathbf{D_{o2}})} & \cdots & \frac{\partial \mathbf{E_o}(\omega_\mathbf{f})}{\partial vec(\mathbf{D_{on}})} \end{bmatrix} && (15)\\
&= -\mathbf{C_o}(\omega_\mathbf{f})^{-\mathbf{1/2}}[(\mathbf{N_o}(\omega_\mathbf{f})\mathbf{D}(\omega_\mathbf{f})^{-\mathbf{1}}) \otimes \mathbf{D}(\omega_\mathbf{f})^{-\mathbf{T}}] \begin{bmatrix} I_{N_i^2} z^n & \cdots & I_{N_i^2} z & I_{N_i^2} \end{bmatrix} && (16)\\
\mathbf{Y_o}(\omega_\mathbf{f}) &= \begin{bmatrix} \frac{\partial \mathbf{E_o}(\omega_\mathbf{f})}{\partial vec(\mathbf{N_{o1}})} & \frac{\partial \mathbf{E_o}(\omega_\mathbf{f})}{\partial vec(\mathbf{N_{o2}})} & \cdots & \frac{\partial \mathbf{E_o}(\omega_\mathbf{f})}{\partial vec(\mathbf{N_{on}})} \end{bmatrix} && (17)\\
&= -\mathbf{C_o}(\omega_\mathbf{f})^{-\mathbf{1/2}}\mathbf{D}(\omega_\mathbf{f})^{-\mathbf{1}} \begin{bmatrix} I_{N_i} z^n & \cdots & I_{N_i} z & I_{N_i} \end{bmatrix} && (18)
\end{aligned}$$

with $\otimes$ the kronicker product.

3.2 Reduced Normal Equations

Taking into account the structure of the Jacobian matrix the normal equation can be written as

$$\mathbf{J_m^H J_m vec}(\mathbf{\Delta\Theta_m}) = -\mathbf{J_m^H vec}(\mathbf{E}) \tag{19}$$

$$\begin{bmatrix} \mathbf{R_1} & 0 & \dots & 0 & \mathbf{S_1} \\ 0 & \mathbf{R_2} & \dots & 0 & \mathbf{S_2} \\ \vdots & \vdots & \ddots & \vdots & \vdots \\ 0 & 0 & \dots & \mathbf{R_{N_o}} & \mathbf{S_{N_o}} \\ \mathbf{S_1^H} & \mathbf{S_2^H} & \dots & \mathbf{S_{N_o}^H} & \sum_{o=1}^{N_o} T_o \end{bmatrix} \begin{bmatrix} \Delta vec(\mathbf{N_1}) \\ \Delta vec(\mathbf{N_2}) \\ \vdots \\ \Delta vec(\mathbf{N_{N_o}}) \\ \Delta vec(\mathbf{D}) \end{bmatrix} = - \begin{bmatrix} \mathbf{V_1} \\ \mathbf{V_1} \\ \vdots \\ \mathbf{V_{N_o}} \\ \sum_{o=1}^{N_o} \mathbf{W_o} \end{bmatrix} \tag{20}$$

with $\mathbf{D} = \begin{bmatrix} D_1 & \dots & D_n \end{bmatrix}$, $\mathbf{N_o} = \begin{bmatrix} N_{o1} & \dots & N_{on} \end{bmatrix}$ and

$$\begin{aligned}
\mathbf{R_o} &= \mathbf{X_o^H X_o} \in \mathbb{C}^{\mathbf{N_i n} \times \mathbf{N_i n}} && (21)\\
\mathbf{S_o} &= \mathbf{X_o^H Y_o} \in \mathbb{C}^{\mathbf{N_i n} \times \mathbf{N_i^2 n}} && (22)\\
\mathbf{T_o} &= \mathbf{Y_o^H Y_o} \in \mathbb{C}^{\mathbf{N_i n^2} \times \mathbf{N_i^2 n}} && (23)\\
\mathbf{V_o} &= \mathbf{X_o^H E_o} \in \mathbb{C}^{\mathbf{N_i n} \times \mathbf{1}} && (24)\\
\mathbf{W_o} &= \mathbf{Y_o^H E_o} \in \mathbb{C}^{\mathbf{N_i n^2} \times \mathbf{1}} && (25)\\
& && (26)
\end{aligned}$$

It can be shown that the submatrices $\mathbf{R_o}, \mathbf{S_o}$ and $\mathbf{T_o}$ have a predefined so-called block toeplitz structure. Therefore only one column and row of the submatrices must calculated to construct the total submatrices. This reduces both calculation time and memory requirements. Furthermore the individual elements of these submatrices can be calculated by the use of fast signal processing techniques like e.g. the Fast Fourier Transformation.

3.3 Solving the Reduced Normal Equations

The major gain in calculation time comes from the use of the structure of the normal equations. Using some elimination and substitution procedures yields to

$$\begin{aligned}
\sum_{o=1}^{N_o} (\mathbf{T_o} - \mathbf{S_o^H R_o^{-1} S_o}) \mathbf{\Delta vec}(\mathbf{D}) &= -\sum_{o=1}^{N_o} (\mathbf{W_o} - \mathbf{S_o^H R_o^{-1} V_o}) && (27)\\
\Delta vec(\mathbf{N_o}) &= -\mathbf{R_o^{-1}}(\mathbf{S_o \Delta vec}(\mathbf{D}) + \mathbf{V_o}) && (28)
\end{aligned}$$

Solving 27 leads to the update of the denominator coefficients, while the numerator coefficients are obtained by substitution of 27 in 28. In this way the inversion of the matrix $J^H J$ can be avoided leading to significant reduction is calculation time.

3.4 Deriving confidence intervals

A good approximation of the covariance matrix of the ML estimate $\hat{\theta}_{ML}$ is given by [13], [6]

$$cov(vec(\hat{\theta}_{ML})) = [J_m^H J^H]^{-1} \tag{29}$$

with J_m the Jacobian matrix evaluated in the last iteration step of the Gauss-Newton algorithm. As one is mainly interested in the uncertainty on the resonance frequencies and damping ratios, only the covariance matrix of the denominator coefficients is in fact required. Starting from 29, one can show by using the matrix inversion lemma, that this matrix is given by

$$cov(vec(\hat{\mathbf{D}}_{ML})) = [\sum_{o=1}^{N_o} \mathbf{T_o} - \mathbf{S_o^H R_o^{-1} S_o}]^{-1} \tag{30}$$

Hence, it is not necessary to invert the full matrix occuring in 29. From 30, one can compute the uncertainty on the poles (or resonance frequencies and damping ratios) using a generalization of [5] from scalar polynomials to square matrix polynomials.

3.5 Robustification of the p-MLFD

The robustness of the p-MLFD algorithm can be improved by using a logarithmic equation error.

$$\mathbf{E_o}(\theta, \omega_\mathbf{f}) = \mathbf{log}\left(\mathbf{H}(\omega_\mathbf{f})^\mathbf{T}\right) - \mathbf{log}\left(\mathbf{D}(\omega_\mathbf{f})^{-\mathbf{T}}\mathbf{N}(\omega_\mathbf{f})^\mathbf{T}\right) \tag{31}$$

The covariance matrix reduces in this case to

$$\mathbf{C_{log,o}}(\omega_\mathbf{f}) = \begin{bmatrix} H_{o1} & 0 & \dots & 0 \\ 0 & H_{o1} & \dots 0 & \\ \vdots & \vdots & \ddots & \vdots \\ 0 & 0 & 0 & H_{oN_i} \end{bmatrix}^\mathbf{H} \mathbf{C_o} \begin{bmatrix} H_{o1} & 0 & \dots & 0 \\ 0 & H_{o1} & \dots 0 & \\ \vdots & \vdots & \ddots & \vdots \\ 0 & 0 & 0 & H_{oN_i} \end{bmatrix} \tag{32}$$

with C_o defined by 8. This logarithmic estimator is 'practically' consistent, robust to the noise assumptions made as well as to outliers, and can handle measurements with a large dynamical range [4]. To speed up this logarithmic based approach similar techniques can be used as explained in previous paragraphs.

3.6 Practical implementation and Remarks

In this section some practical issues and remarks are discussed about the algorithm.

- The solution of the p-MLFD method is exactly the maximum likelihood solution if the noise on the FRFs over different outputs is uncorrelated. This is exactly the case for roving hammer tests where the number of reference sensors can be seen as the number of inputs and the number of outputs is equal to the number of locations where on hits with the hammer. In case this noise assumption is not true (e.g. shaker tests) the algorithm is still consistent, but looses a bit of efficiency. It can be shown that the p-MLFD method is always consistent even in the case no noise information is used. The use of a correct noise assumption and information for the p-MLFD improves the efficiency of the algorithm. In [15] a detailed discussion is given about how to obtain the variances and covariances on your FRFs, estimated by e.g. the H_1 method.
- In the case no a prior noise method is available, one has to make an assumption for the noise model. In case one assumes to have white additive noise on the FRFs, the covariance matrix $C_o(\omega_f)$ is equal to the unity matrix I_{N_i}. The assumption of relative noise on the FRFs corresponds with $C_{log,o}(\omega_f)$ equal to the unity matrix I_{N_i}. From our experience we advice in absence of any noise information to use the logarithmic version of the p-MLE with the assumption of relative noise.

- Many EMA algorithms suffer from bad numerical condition in case high order models are estimated. All the mentioned algorithms in this paper, p-MLFD, MLFD, p-LSCF and LSCF method deal with problem by re-scaling the frequencies between 0 and 1. By doing this, the basic functions of the polynomials $\Omega_r(\omega) = e^{j\omega T_s r}$ become orthonormal and hence this results in a well conditioned problem.
- Since both the p-MLFD as the MLFD are optimization methods and thus iterative, they require good starting values. These starting values are respectively obtained by the p-LSCF and LSCF methods. To ensure convergence the Gauss-Newton algorithm is implemented by a Levenberg-Marquard approach [3]. Finally it should be mentioned that in the case of single input measurements, the right matrix fraction model and the common denominator model are equal and hence the p-MLFD and p-LSCF method result respectively in exactly the same estimates as the MLFD and LSCF method.

4 INDUSTRIAL APPLICATIONS

The presented algorithm has several applications in automotive, civil and aerospace applications. The discussed case studies show the advantage of the presented p-MLFD method.

4.1 Civil Engineering: Bridge testing

The use of output-only identification techniques has several applications in civil engineering. Instead of using the FRFs as a basis to start the identification, OMA techniques start from the auto and cross power densities $G_{YY_{oi}}$of the response measurements instead of starting from FRFs.

$$G_{YY_{oi}}(\omega_f) = \frac{1}{N_b}\sum_{b=1}^{N_b} Y_{ob}(\omega_f)Y_{oi}(\omega_f)^* \tag{33}$$

with N_b the number of blocks in which the time data is divided and N_i the number of reference signals. In [8] it is shown how the MLFD method, based on common denominator model, deals with output-only data. Since it is recommended to use several reference sensors, the use of the poly-reference p-MMFD algorithm is preferred.

Figure 1 gives a view of the measured span. The measurement were done in two different patches with two reference acceleration measurements. A periodogram approach is used to calculate the auto and power spectral densities [8], [11]. In a low frequency band

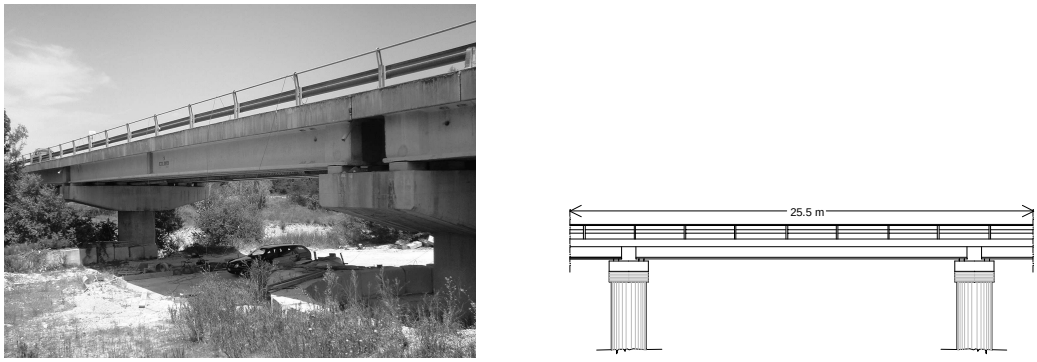

Figure 1: Picture of the instrumented span of the 8-span bridge overpassing the Vomano river

between 4Hz and 6Hz a first bending and torsion mode was identified with a model order of 10 modes and 30 p-MLFD iterations. Figure 2 shows the stabilization diagram, a synthesized FRF and both identified modes. In the higher frequency band clearly 5 other higher bending and torsion modes are identified. Figure 3 shows the stabilization chart and the increased accuracy of the p-MLFD compared to the p-LSCF algorithm. The normalized error between a measured $H_{oi}(\omega_k)$ and the synthesized FRF $\hat{H}_{oi}(\omega_k)$ is defined as

$$E_{H_{oi}} = \frac{\sum_{k=1}^{N_f} |\hat{H}_{oi}(\omega_k) - H_{oi}(\omega_k)|^2}{\sum_{k=1}^{N_f} |H_{oi}(\omega_k)|^2} \tag{34}$$

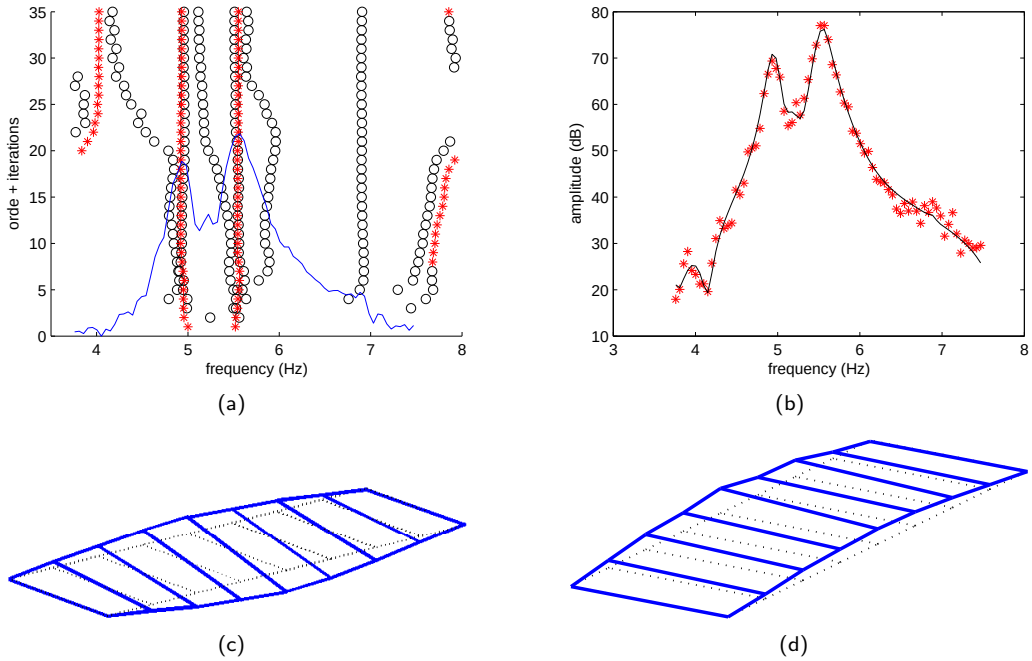

Figure 2: p-MLFD results a) Stabilization diagram (asterix: stable pole, circle: unstable pole), b) A synthesized power density (asterix: measurement, full line: p-MLFD), c) first torsion mode, d) first bending mode

The mean error over all references i and outputs o is reduced by a factor 10 by using the p-MLFD algorithm compared to p-LSCF algorithm.

4.2 Automotive Engineering: Fully Trimmed Car

In automotive engineering EMA is considered as a "commodity" tool and accurate models are needed for modelling and finite element updating.

A MIMO test excited a fully trimmed Porsche in 4 different locations by shakers. The accelerations were measured in 154 locations spread all over the car. The FRFs are estimated by the H_1 method [10]. Since no covariances were available in the data set, the logarithmic implementation of both the p-MLFD and the MLFD used with a weighting $C_{log,o}(\omega_f) = I_{N_i}$. A comparison was made between the p-MLFD, MLFD, p-LSCF, LSCF and Least Squares Complex Exponential (LSCE) algorithms on basis of the estimated modal model.

A model order of 26 modes was used to identify the modal parameters in frequency band from 3Hz to 30Hz. Table 2 compares the mean errors over all input-output relations and de mean correlation for the different algorithms with the correlation between the synthesized FRF H_{oi} and the measured FRF $\hat{H}_{oi}$ defined as

$$CR_{H_{oi}} = \frac{\left|\sum_{f=1}^{N_f} \hat{H}_{oi}(\omega_f) H_{oi}^*(\omega_f)\right|^2}{\left(\sum_{f=1}^{N_f} \hat{H}_{oi}(\omega_f)\hat{H}_{oi}^*(\omega_f)\right)\left(\sum_{f=1}^{N_f} H_{oi}(\omega_f)H_{oi}^*(\omega_f)\right)} \tag{35}$$

It is clear that the p-MLFD gives the best results in terms of the fit of the modal model. For the least squares algorithms the p-LSCF method outperforms both the LSCF and LSCE algorithms. It should be mentioned that both the p-MLFD as the MLFD algorithm resulted in perfect fits of respectively the right-matrix fraction model and the common-denominator model. Nevertheless the common denominator based algorithms LSCF and MLFD loose quality by converting the common denominator model to the modal model by reducing the residues to a rank-one matrix using an SVD. Other examples [1] and [12] proof this fact. It seems that this fact of loosing quality by transferring common denominator models into modal models tends to be more problematic for

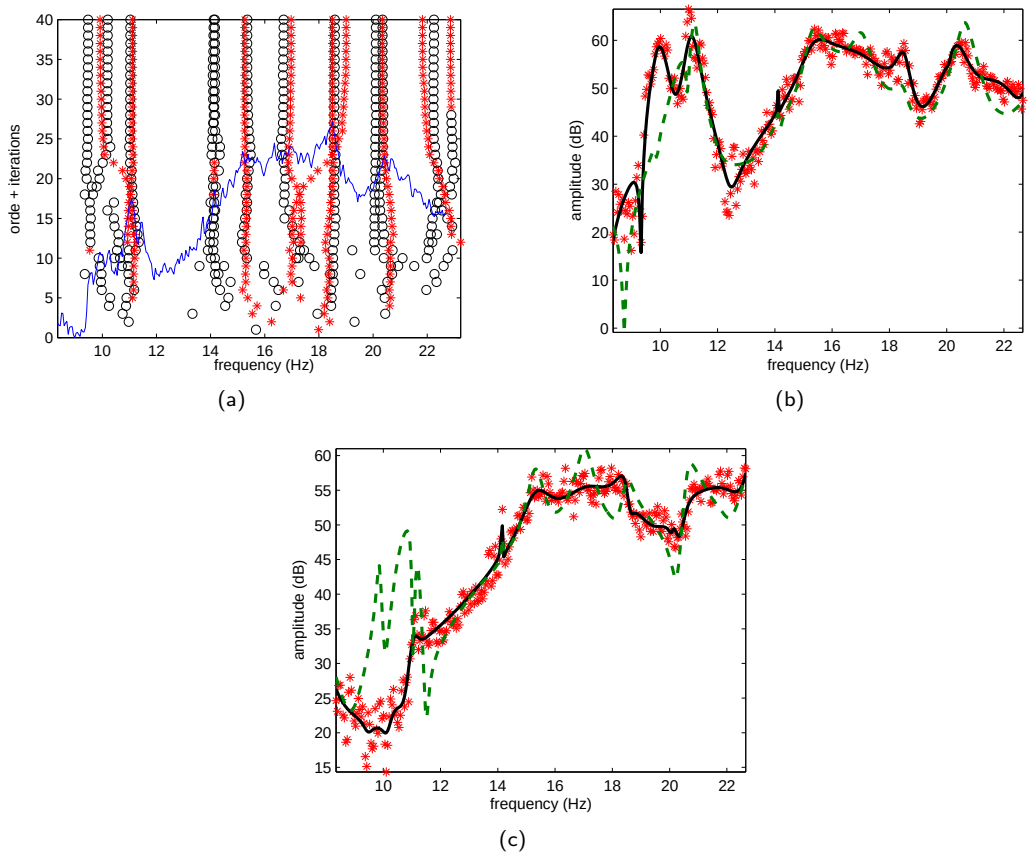

Figure 3: p-MLFD results a) Stabilization diagram (asterix: stable pole, circle: unstable pole), b and c) Synthesized power densities (asterix: measurement, full line: p-MLFD, dashed line p-LSCF)

Table 2: Comparison between the different algorithms

algorithm	mean error	mean correlation
p-MLFD	1.41%	98.64%
MLFD	21.48%	85.47%
p-LSCF	9.92%	91.20%
LSCF	28.36%	81.94%
LSCE	18.53%	83.31%

highly-damped cases (damping ratios $> 2\%$). By using a right matrix fraction model like the p-LSCF and MLFD a rank-one residue matrix is inherent to the model and as a result less quality is lost by converting the model into a modal model.

Figure 5 shows the stabilization diagram obtained by the p-MLFD method for a model with 26 poles and 50 iterations of the algorithm. Table 3 shows the estimated natural frequencies and their damping ratios. This proves that the p-MLFD method is capable to deal with high modal densities and highly damped structures.

In fact, the p-MLFD optimizes the estimated model in a Maximum Likelihood sense by optimizing the resonance frequencies, damping ratios, mode shapes and participation factors. The common denominator based MLFD algorithm optimizes the model by optimizing the the resonance frequencies, damping ratio and residues, while there is no guarantee that the residue matrices are of rank one. Instead of optimizing the modal parameters, the MLFD algorithm uses this extra freedom in the model for fine tuning its model.

Table 3: Natural Frequencies and damping ratios estimated by p-MLFD

frequency (Hz)	damping ratio (%)
4.05	5.80
4.29	7.49
4.72	6.55
6.04	4.29
8.59	6.80
14.69	5.75
15.74	8.30
17.07	5.54
18.34	5.09
20.79	4.01
21.82	3.07
22.43	4.29
25.15	3.03
25.93	3.03
26.93	6.00

4.3 Flight Flutter Testing

Aircraft and winged-launch vehicles must be free from aerodynamic instabilities such as flutter to ensure safe operation. Flutter is a dynamic instability that involves coupling of aerodynamic, elastic and inertial forces of the structure. During flight the structure extracts energy from the airstream. At speeds larger than the critical airspeed, the energy dissipated is less than the available structural damping and the motion is divergent. The airworthiness regulation requires that a full-scale aircraft is demonstrated free from flutter by a flight flutter test. In these tests natural frequencies and modal damping ratios are estimated for different flight conditions. Most common approaches track the damping ratios of the different flight conditions, which are then extrapolated in order to determine whether it is save to proceed to the next flight point. Flutter occurs when one of the damping values tends to become negative. The speed at which such an instability takes place is called the flutter speed and is one of the most important design parameters for an aircraft wing. Flight flutter testing continues to be a challenging research area because of the concerns with costs, time and safety in expanding the envelope of new or modified aircrafts. The aerospace industry desires to decrease the flight flutter testing time for practical, economical and safety reasons and to improve the accuracy and reliability of the parameter estimation.

Figure shows compares the synthesized FRFs from the p-MLFD and p-LSCF algorithms to the measured FRFs of a commercial airplane which was excited at 2 locations during flight. The vibration response was measured at 11 different locations $120s$. In-Flight test data is typically characterized by large noise levels due to turbulence, non-linearities and a relative small data set (small amount of averages to estimate the FRFs). It is clear that for these relative noisy measurements the p-MLFD outperforms the p-LSCF approach.

5 CONCLUSIONS

The proposed poly-reference maximum likelihood frequency domain (p-MLFD) modal parameter identification algorithm results in very accurate modal parameters. The p-MLFD is capable to deal with high modal densities and highly damped systems. It is shown by several examples that the presented method outperforms common-denominator model based identification algorithms in terms of the quality of the modal parameters. In contrast to least squares based algorithms, the presented maximum likelihood implementation is capable to deal with noisy FRFs. The applicability of the presented modal identification method is shown by different examples.

ACKNOWLEDGEMENTS

The financial support of the Fund for Scientific Research (FWO Vlaanderen), the Concerted Research Action "OPTIMech" of the Flemish Community; the Research Council (OZR) of the Vrije Universiteit Brussel (VUB) are gratefully acknowledged. The first author holds a Research Assistant Grant of the Fund for Scientific Research - Flanders (Belgium)(F.W.O. - Vlaanderen) at the mechanical engineering department of the Vrije Universiteit Brussel.

REFERENCES

[1] H. Van der Auweraer, P. Guillaume, P. Verboven, and S. Vanlanduit. Application of a fast-stabilizing frequency domain parameter estimation method. *Journal of Dynamic Systems, Measurement, and Control*, 123:651–658, 2001.

[2] B. Cauberghe, P. Guillaume, and B. Dierckx. Identification of modal parameters from inconsistent data. In *Proceedings of the 20th International Modal Analysis Conference*, Los Angeles (CA), February 2002.

[3] B. Cauberghe, P. Guillaume, P. Verboven, and E. Parloo. Modal parameter estimation from output-only measurements in presence of transient phenomena. In *Proceedings of the 25th International Seminar on Modal Analysis*, Leuven (Belgium), September 2002.

[4] P. Guillaume, R. Pintelon, and J. Schoukens. Robust parametric transfer function estimation using complex logarithmic frequency response data. *IEEE Transactions on Automatic Control*, 40(7), 1995.

[5] P. Guillaume, J. Schoukens, and R. Pintelon. Sensitivity of rooots to errors in the coefficient of polynomials obtained by frequency-domain estimation methods. *IEEE Transactions on Instrumentation and Measurement*, 38(6):1050–1056, 1989.

[6] P. Guillaume, P. Verboven, and S. Vanlanduit. Frequency-domain maximum likelihood identification of modal parameters with confidence intervals. In *Proceedings of the 23th International Seminar on Modal Analysis*, Leuven (Belgium), September 1998.

[7] P. Guillaume, Peter Verboven, S. Vanlanduit, H. Van der Auweraer, and B. Peeters. A poly-reference implementation of the least-squares complex frequency domain-estimator. In *Proceedings of the 21th International Modal Analysis Conference*, Kissimmee (Florida), February 2003.

[8] L. Hermans, H. Van der Auweraer, and P. Guillaume. A frequency-domain maximum likelihood approach for the extraction of modal parameters from output-only data. In *Proceedings of the 23th International Seminar on Modal Analysis*, Leuven (Belgium), September 1998.

[9] W. Heylen, S. Lammens, and P. Sas. *Modal Analysis Theory and Testing*. K.U.Leuven, 1998.

[10] N.M. Maia and J.M. Silva. *Theoretical and Experimental Modal Analylis*. John Wiley & Sons, 1997.

[11] E. Parloo. *Application of Frequency-domain System Identification in the Field of Operational Modal Analysis*. Ph.D. Thesis, Vrije Universiteit Brussel, Departement of Mechanical Engineering, 2003.

[12] B. Peeters, P. Guillaume, B. Cauberghe, P. Verboven, and H. Van der Auweraer. Automotive and aerospace applications of a new fast-stabilizing polyreference frequency-domain parameter estimation method. In *Proceedings of the 21th International Modal Analysis Conference*, Dearborn (US), January 2004.

[13] R. Pintelon and J. Schoukens. System identification: A frequency domain approach. *IEEE Press*, 2001.

[14] Kailath T. *Linear Systems*. Prentice Hall, 1980.

[15] P. Verboven. *Frequency-domain System Identification for Modal Analysis*. Ph.D. Thesis, Vrije Universiteit Brussel, Departement of Mechanical Engineering, 2002.

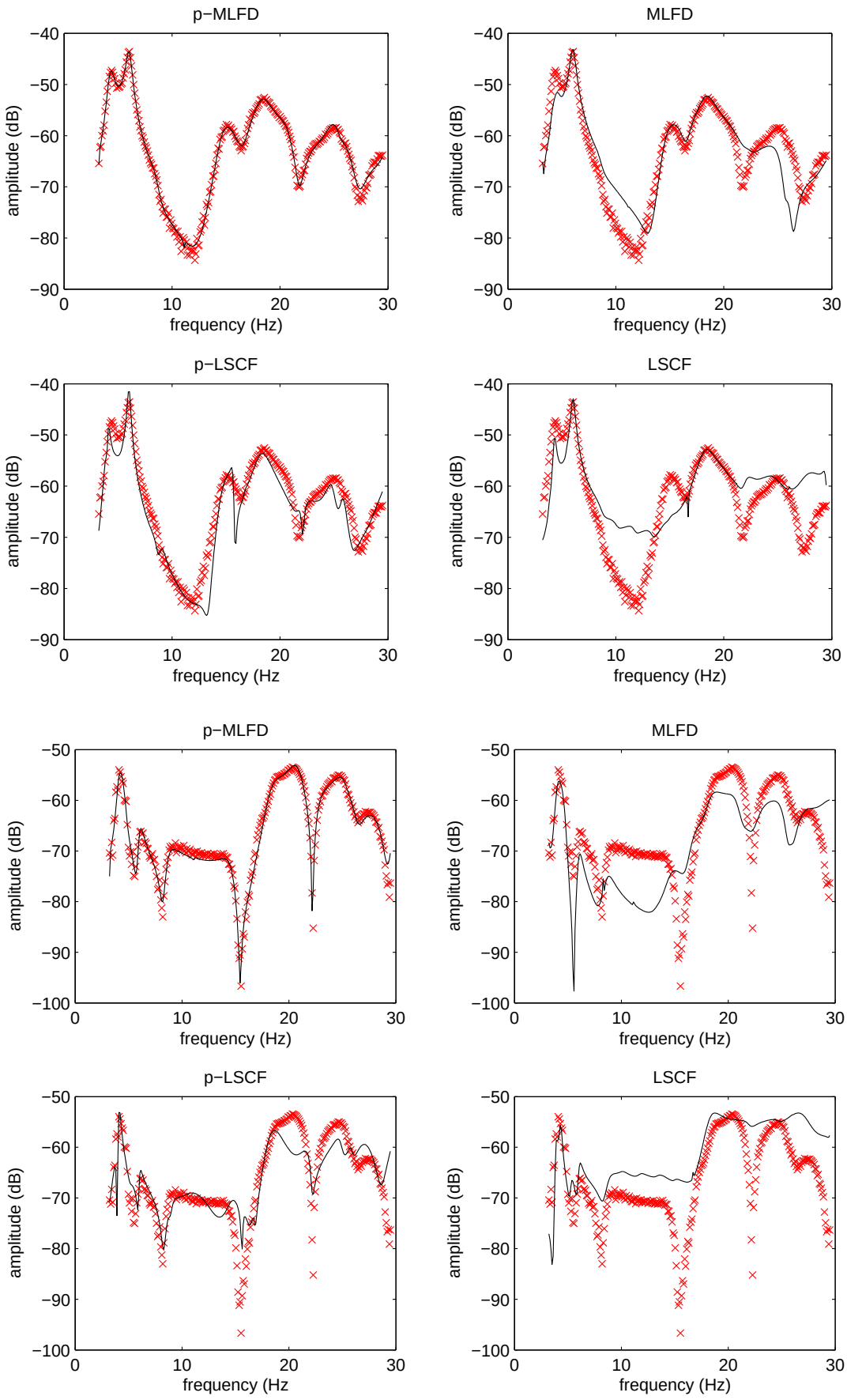

Figure 4: Comparison between the modal model obtained by the p-MLFD, MLFD, p-LSCF and LSCF algorithm for two FRFs. (cross: measurement, full line: estimated modal model)

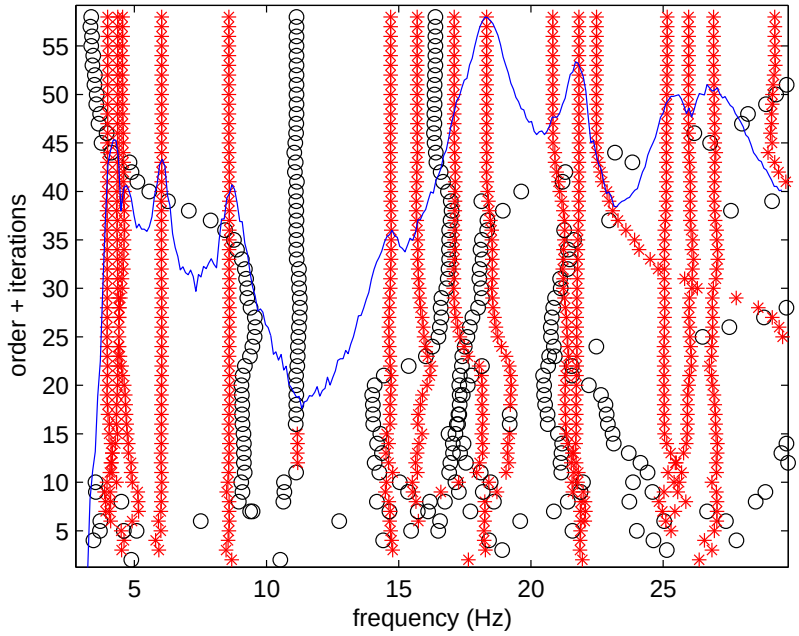

Figure 5: Stabilization chart of the p-MLFD for measurements on a fully trimmed car (asterix: stable pole, circle: unstable pole)

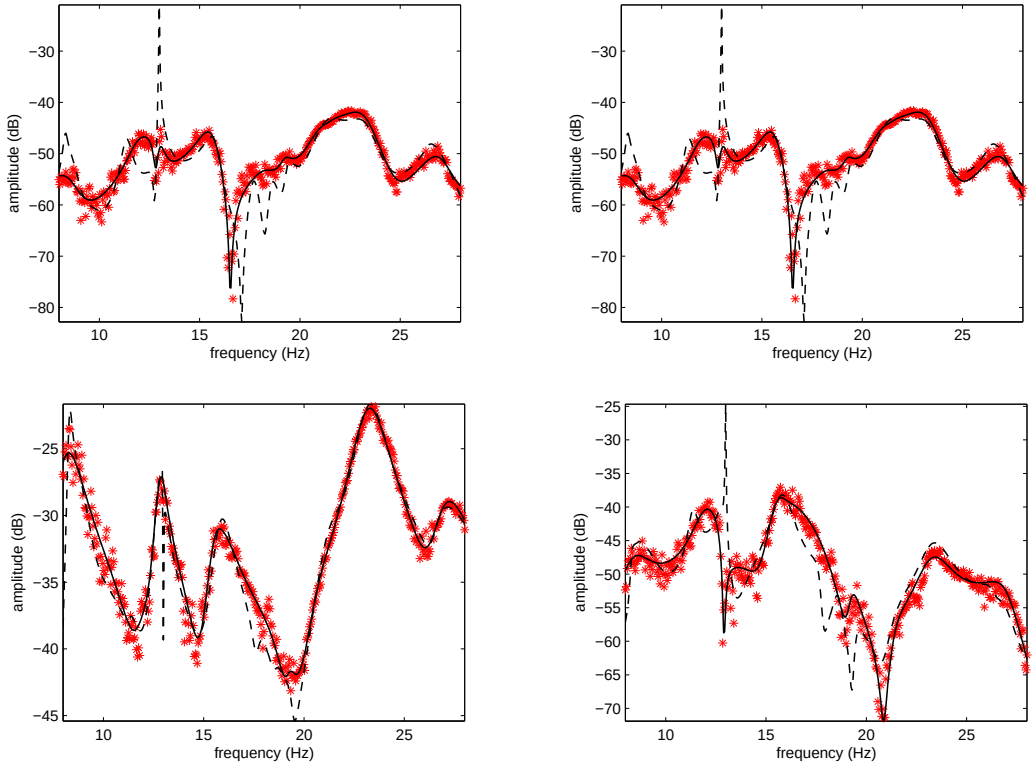

Figure 6: p-MLFD applied on in flight-flutter measurements (cross: measurement, full line: p-MLFD, dashed line: p-LSCF)